Research in Pharmaceutical Sciences, June 2025; 20(3): 416-433
Received: 18-03-2024
Peer Reviewed: 07-08-2024
Revised: 16-01-2025
Accepted: 18-01-2025
Published: 17-06-2025

School of Pharmacy & Pharmaceutical Sciences
Isfahan University of Medical Sciences

Original Article

Protective effects of curcumin/magnesium oxide nanoparticles on ketamine-induced neurotoxicity in the mouse hippocampus

Mahsa Salehirad[1], A. Wallace Hayes[2,3], Majid Motaghinejad[4,*], and Mina Gholami[5]

[1]*Department of Pharmaceutical Chemistry, Faculty of Pharmaceutical Chemistry, Tehran Medical Sciences, Islamic Azad University, Tehran, I.R. Iran.*
[2]*Institute for Integrative Toxicology, Michigan State University, East Lansing, MI, USA.*
[3]*Center for Environmental Occupational Risk Analysis and Management, College of Public Health, University of South Florida, Tampa, FL, USA.*
[4]*Chronic Respiratory Disease Research Center (CRDRC), National Research Institute of Tuberculosis and Lung Diseases (NRITLD), Shahid Beheshti University of Medical Sciences, Tehran, I.R. Iran.*
[5]*College of Medicine, Shahid Beheshti University of Medical Sciences, Tehran, I.R. Iran.*

Abstract

Background and purpose: Nanotechnology can improve drug delivery by enhancing cell selectivity, releasing at specific target sites, and improving bioavailability while reducing adverse events and potential treatment costs. The current study aimed to synthesize curcumin/magnesium oxide (Cur/MgO) nanoparticles (NPs) and evaluate their neuroprotective effects in a mouse model of ketamine-induced neurotoxicity.
Experimental approach: XRD, FE-SEM, and a particle size analyzer determined the average crystalline and particle sizes. UV-Vis examined absorption patterns, and FT-IR spectroscopy analyzed the functional groups involved in the reaction. To evaluate the effectiveness of Cur/MgO NPs on ketamine-induced neurotoxicity, male BALB/c mice were divided into 7 groups and received the following treatments (intraperitoneally, daily for 2 weeks). Groups 1 and 2 received normal saline (0.2 mL) and ketamine (25 mg/kg). Group 3 received curcumin (40 mg/kg) and ketamine (25 mg/kg). Groups 4-6 received ketamine (25 mg/kg) and Cur/MgO NPs (10, 20, and 40 mg/kg). Group 7 received MgO (5 mg/kg) and ketamine (25 mg/kg). Finally, the hippocampal tissues were examined morphologically and analyzed for oxidative stress, inflammation, apoptotic markers, and mitochondrial quadruple complex enzymes.
Results/Findings: Both Cur/MgO NPs and curcumin reduced IL-1β, TNF-α, Bax, and MDA levels and GSSG content and increased GSH, Bcl-2, GPx, GR, and SOD. Cur/MgO NPs and curcumin also increased mitochondrial quadruple complex enzymes and inhibited histological changes in the dentate gyrus and CA1 hippocampus areas in ketamine-induced neurotoxicity.
Conclusion and implications: Cur/MgO NPs were more neuroprotective against the ketamine-induced histomorphological changes, inflammation, apoptosis, and oxidative stress than curcumin alone.

Keywords: Curcumin/magnesium oxide nanoparticles; Ketamine; Mouse hippocampus; Neurodegeneration.

INTRODUCTION

Nanotechnology can improve drug delivery while reducing adverse events and potential treatment costs. Additional nanotechnology improvements include cell selectivity, release at specific target sites, and enhanced bioavailability from increased drug solubility (1,2). Magnesium is the second most abundant intracellular cation after potassium and is a noncompetitive antagonist for the N-methyl-D-aspartate receptor (NMDA). The NMDA receptor is blocked and downregulated by excess magnesium (3).

*Corresponding author: M. Motaghinejad
Tel: +98-2126109991, Fax: +98-2126109484
Email: Dr.motaghinejad6@gmail.com

Access this article online	
	Website: http://rps.mui.ac.ir
	DOI: 10.4103/RPS.RPS_5_23

Magnesium oxide nanoparticles (MgO NPs) influenced the regulation of neuronal cell activity in several mammalian cell types (4). Because of their size, formation, and structure, MgO NPs have the potential to be functional drugs (5). MgO NPs reduced pain and inflammation in mice through central and peripheral pathways (6). Additionally, Moeini-Nodeh *et al.* showed that MgO NPs have both antiapoptotic and antioxidative effects (7).

Curcumin (Cur) is a traditionally used Eastern medicinal ingredient with centuries of safe use and efficacy (8-12). Curcumin is the principal curcuminoid in turmeric, a popular Indian spice derived from the rhizome of *Curcuma longa* (13). Curcumin's antioxidant, anti-inflammatory, anti-proliferative, antiseptic, analgesic, anti-malarial, antitumoral, apoptosis-inducing, and anti-angiogenesis properties have been reported (14). All appear to involve the inhibition of nuclear factor kappa B (NFk B) signaling, which lowers pro-inflammatory cytokines interleukin (IL)-1, IL-6, and tumor necrosis factor-alpha (TNF-α) (15). In an alcoholic animal neuropathy model, Cur antagonized the cellular consequences of oxidative stress by preventing DNA damage (16). Curcumin may be a promising remedy for certain neurodegenerative diseases (15, 17,18).

In obstetric and pediatric patients, ketamine, an NMDA receptor antagonist, is used for its analgesic and anesthetic effects (19). Ketamine has been reported to promote neuronal cell death and neurodegeneration, but the mechanism underlying its harmful effects remains elusive (20,21). Ketamine increased lipid and protein peroxidation, enhanced free radical formation and activities, and reduced glutathione and antioxidant activity in humans and animals (9,22). Ketamine increased several neuro-inflammatory pathways, cytokine, chemokine, and inflammatory-related signaling pathways in mice and induced cell death in a PC12 cell line (22-24).

Ketamine, however, has the potential for abuse due to its hallucinogenic and other reinforcing characteristics (25,26). Ketamine abuse or continuous administration activates apoptosis and cell death signaling pathways, such as necrosis and autophagy, in adult neural stem cells and PC 12 cells (27,28). The frequencies with which practitioners prescribe KET and the frequency of its illicit trade for recreational use have contributed to increased abuse (25,26).

In the current study, Cur-MgO NP was synthesized to evaluate its neuroprotective effects against ketamine-induced neurotoxicity in mouse hippocampal cells, emphasizing its impact on mitochondrial function, anti-inflammatory, antioxidant, and anti-apoptotic pathways.

MATERIALS AND METHODS

Materials

Ketamine, lithium, potassium hydroxide, and magnesium nitrate hexahydrate (Mg $(NO_3)_2$ $6H_2O$) were purchased from Sigma Aldrich (US). Merck supplied the curcumin. Normal saline was the control and the solvent for the test chemicals. The test kits were purchased from DNA Biotech Co. (Tehran, Iran). All reagents were of analytical grade.

Nanoparticle synthesis

Cur/MgO nanoparticles were synthesized as follows. Fifty mg of Cur was dissolved in 50 mL of ddH_2O at 80 °C. The solubilized Cur was added to a magnesium nitrate solution (Mg $(NO_3)_2$, 50 mL, 0.1 M), resulting in a yellowish-colored solution. The solution was refluxed at 85-90 °C for 2 h. When the refluxed solution was cooled to 40 °C, 5 mL of KOH (0.2 M) was gradually added, leading to an orange-yellow gel-like suspension. This suspension was centrifuged at 10,000 rpm, and the residue was washed with acetone and water until no yellow color (Cur) was observed. The nanoparticles were thoroughly washed with acetone after synthesis to remove unreacted materials. The resulting Cur/MgO nanoparticles were vacuum-dried at ambient temperature. The nanoparticles were dissolved in normal saline, placed in an ultrasonic bath for 15 min, and then stored at pH 8.3 to maintain the stability of the nanoparticles (29-31).

Nanoparticle characterization

Field emission scanning electron microscope (FE-SEM), X-ray diffractometer (XRD), Fourier transform infrared (FT-IR) spectral analysis, and UV-Vis spectra assessed the nanostructure's particle size, morphology, and chemical composition. FT-IR spectra were obtained using a PerkinElmer instrument, and a Philips powder diffractometer was used to determine the X-ray diffraction pattern. The scanning rate for the diffractometer was in the range of 10-80°. To confirm chemical formation, a double-beam spectrophotometer measured the UV-visible

spectrum. FE-SEM analyzed the morphology and particle dispersion of the nanoparticles, and the chemical composition of the Cur/MgO nanoparticle was evaluated using energy-dispersive X-ray spectroscopy. Uncorrected melting points were determined using a capillary tube and a B510K melting point instrument. These techniques provide a comprehensive understanding of the characteristics of the synthesized nanostructure (29-31).

In-vivo study

Animals

Fifty-six male BALB/c mice weighing 25-30 g were obtained from the Animal Experimental Research Center, Iran University of Medical Sciences. The mice had access to pellet feed (Parsfeed Co., Tehran, Iran) and water in a controlled environment (room temperature: 22 ± 0.5 °C; relative humidity: 6-40%; 12/12-h light/dark cycles). Animals (8) were grouped and housed in wire-bottom cages and monitored for signs of toxicity pre-treatment and continuously during the study.

Ethics statement

The research protocol (Ethic No I.R.SBMU.NRITLD.REC.1402.093) adhered to the Animal Ethics and Welfare Guidelines of the Shahid Beheshti University of Medical Sciences Animal Care and Use guidelines and the ARRIVE procedure for the ethical treatment of the animals (32).

Experimental procedure

After two week of acclimatization, the mice were randomly divided into six experimental and one control groups and dosed i.p. daily for 2 weeks (Fig. 1). Group 1 (control) received 0.2 mL of normal saline; Group 2, animals received ketamine (25 mg/kg); Group 3, animals received 40 mg/kg Cur and 25 mg/kg ketamine; Groups 4-6 received ketamine (25 mg/kg) and Cur/MgO NPs (10, 20, or 40 mg/kg); Group 7 received 5 mg/kg MgO and ketamine (25 mg/kg). A schematic diagram of the overall experimental protocol and timeline is depicted in Fig. 2. The interval between injections for mice in groups 3-7 was 1 h. Dose selection for ketamine and Cur was based on the literature (9,12,22,27,28). Cur/MgO NPs doses were selected based on behavioral results in an unpublished/pilot study. The treatment period of 14 days was to ensure sufficient time for the chosen biomarkers to manifest (9,12,22,27,28,33).

Assessment for oxidative stress, inflammation, apoptosis, and mitochondrial respiratory chain enzyme

Measurements of total protein

On day 15, mice were anesthetized with Trapanal (50 mg/kg, i.p.), and the brains were removed. The hippocampus was carefully separated into its two hemispheres, and the right hemisphere was homogenized in a cold buffer, followed by centrifugation at 450 g for 10 min. The buffer contained 4-morpholinepropanesulfonic acid (25 mM), sucrose (400 mM), magnesium chloride (4 mM), ethylene glycol tetraacetic acid (0.05 mM), and the pH of the solution was 7.3. Subsequently, the samples underwent a second 10-min centrifugation at 12,000 *g*. The resulting sediment was resuspended in the buffer and stored at 0 °C until analyzed.

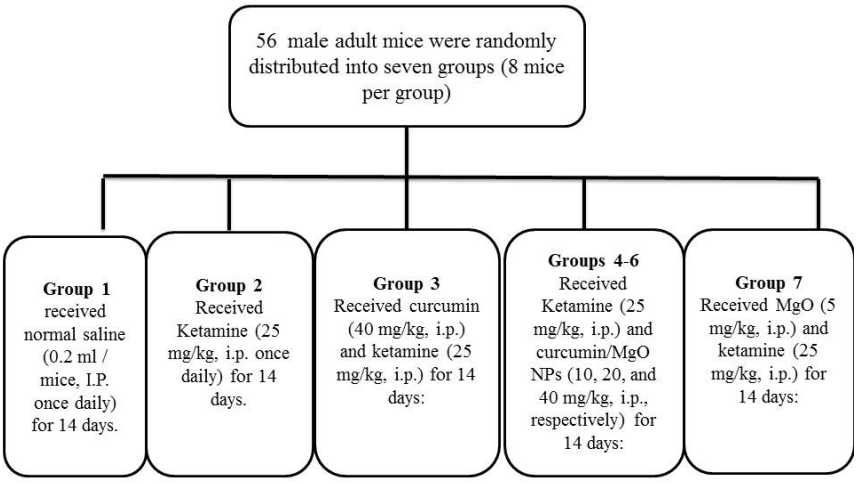

Fig. 1. Schematic illustration of experimental grouping.

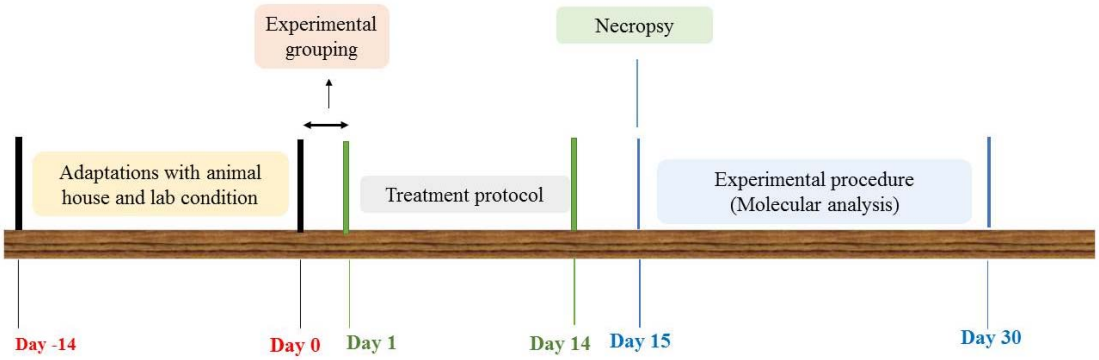

Fig. 2. Timeline for experimental procedure and evaluation.

Bio-Rad CA DC protein assay kits (Providence, RI, USA) were employed to measure the concentration of brain-derived neurotrophic factor (BDNF), cAMP-response element binding protein (CREB), TNF-α, IL-1, B-cell lymphoma 2 (Bcl-2), Bcl-2 associated X-protein (Bax), super oxide dismutase (SOD), glutathione peroxidase (GPx), and glutathione reductase (GR).

Total protein was determined using the Bradford method (Bio-Rad, Providence, RI, USA). A serial dilution of bovine serum albumin, ranging from 0.1 to 1.0 mg/mL, was prepared in the homogenization buffer. A standard curve was created. Protein extracts of 10, 15, 20, 25, and 30 µL were added to individual wells along with the Bradford reagent. Absorbance was measured at 630 nm utilizing a plate reader (Hiperion Microplate Reader, MPR4+, Rayto Company, China) (34-36).

Measurements of oxidative stress parameters

Lipid peroxidation level

The primary byproduct of cellular lipid peroxidation is malondialdehyde (MDA). MDA standard (100 µL; DNA Biotech Co., Tehran, Iran) or 100 µL of the tissue homogenate was added to wells of the 96-microwell plate. Sodium dodecyl sulfate lysis solution (100 µL) was added to each well. Thiobarbituric acid reagent (250 µL; DNA Biotech Co., Tehran, Iran) was added, and the mixture was gently shaken and incubated at 95 °C for 45-60 min. Samples were then centrifuged at 1000 *g* for 15 min. n-Butanol (300 µL; DNA Biotech Co., Tehran, Iran) was added to stop the reaction. Samples were centrifuged at 10,000 *g* for 7 min, and the absorbance was read at 532 nm. Results are reported as nmol/mg of protein (37-41).

GSH and GSSG content

GR solution (25 µL, 1X, DNA Biotech Co., Tehran, Iran) and 25 µL of the NADPH solution (1X; DNA Biotech Co., Tehran, Iran) were added separately to 96-well plates to measure reduced and oxidized glutathione (GSH and GSSG). A standard glutathione solution (DNA Biotech Co, Tehran, Iran) or 25 µL of homogenized tissue sample was added to different wells. Chromogen (50 uL, 1X; DNA Biotech Co., Tehran, Iran) was added and the mixture was vigorously blended. Absorbance was measured at 405 nm. The results are reported as nmol/mg of protein (41,42).

SOD activity

A kit from DNA Biotech Co. (Persequor Park, Pretoria, South Africa) was used to assess SOD activity. The first and third blank wells were filled with ddH_2O, and the second blank well was filled with the homogenized tissue solution with a reagent volume of 20 µL. The process included adding a working solution to each well, gently mixing it, and then adding a dilution buffer and an enzyme working solution to specific wells. For 20 min, the solutions were incubated at 37 °C after being thoroughly mixed. Subsequently, the absorbance was measured at 450 nm, and SOD was quantified as units/mL/mg protein (41-43).

GPx activity

The GPx activity in the hippocampal tissue was assessed using a commercial kit from the DNA Biotech Company (Persequor Park, Pretoria, South Africa). The process included the addition of precise volumes of the homogenized tissue solution, assay buffer, reaction solution, and peroxidase substrate solution to the appropriate wells, followed by the measurement of absorbance at 340 nm over 8 min at 25 °C. The results are in mU/mg protein (41-43).

GR activity

The GR activity was assessed using a kit from the DNA Biotech Company (Persequor Park, Pretoria, South Africa). In the presence of NADPH, the reaction involved the transformation of GSSG to GSH. The reaction mixture was thoroughly mixed before measuring the absorbance at 340 nm for 120 s. The outputs are reported as mU/mg protein (41-43).

Mitochondrial complex enzyme chain

The activities of mitochondrial complexes I, II, III, and IV were assessed using commercial kits from the Abcam Co. (Boston, MA, USA). Measurement of NADH oxidation to NAD^+ at 450 nm estimated the function of mitochondrial complex I. For mitochondrial complex II, the assay involved the electron-transfer catalysis of succinate to ubiquinone by measuring absorbance at 550 nm. The activity of mitochondrial complex III was evaluated by determining the conversion rate of CYCS to its reduced form at 600 nm. The function of mitochondrial complex IV was monitored by quantifying the oxidation of the reduced form of CYCS at 550 nm. The results are activity per milligram of protein per minute (44).

Apoptosis and inflammatory protein expression

TNF-α, IL-1β, Bax, Bcl-2, caspase-3, and caspase-7 were estimated using commercial ELISA kits (Genzyme Diagnostics, Cambridge, USA). Sheep anti-mouse IL-1β, TNF-α, Bax, Bcl-2, caspase-3, and caspase-7 polyclonal antibodies (Sigma Chemical Co., Poole, Dorset, UK) were washed three times (0.5 M sodium chloride (NaCl), 2.5 mM sodium dihydrogen phosphate (NaH_2PO_4), 7.5 mM Na_2HPO_4, 0.1% Tween 20, pH 7.2). Ovalbumin solution (100 mL of 1% w/v; Sigma Chemical Co., Poole, Dorset, UK) was added to each well and incubated at 37 C for 1 h. After washing three times, 100 mL of sample or standard was added to each well and incubated at 48 °C for 20 h. After three washes, 100 mL of biotinylated sheep anti-mouse IL-1β or TNF-α antibody (1:1000 dilutions in wash buffer containing 1% sheep serum, Sigma Chemical Co., Poole and Dorset, UK) was added to each well. Following 1 h of incubation and three washes, 100 mL of Avidin-horseradish peroxidase (HRP; Dako Ltd, UK; 1:5000 dilutions in wash buffer) was added to each well, and the plates were incubated for 15 min. After washing three times, 100 mL of 3,3',5,5' tetramethylbenzidine (TMB) substrate solution (Dako Ltd., UK) was added to each well and incubated for 10 min at room temperature. Finally, 100 mL of 1 M H_2SO_4 was added to stop the reaction, and absorbance was read at 450 nm. The results are expressed as ng/mL for TNF-α and IL-1β and as pg/mL for Bax, Bcl-2, caspase-3, and caspase-7 (45,46).

Histopathology

The left hippocampus was processed according to a standard protocol (47,48). Sections with a thickness of 5 µm were stained with hematoxylin and eosin (H&E) and examined (magnification of 400X) using Optikavision morphometry software (Optikavision Pro, Italy). Cell density and shape were compared in an area of 1.30 mm (47-49).

Statistical analysis

The results are reported as means ± SEM calculated by GraphPad PRISM v.6 software (California, USA). An F-test with degrees of freedom was reported for all parameters (6,42). The Kolmogorov-Smirnov test was applied to evaluate the normality of the data, and the normality of all data and variables was confirmed. The homogeneity of variances between two or more groups was assessed by Levene's or Bartlett's tests; the variance between groups was homogeneous. Statistical significance was determined by one-way ANOVA followed by Tukey's post-hoc test to compare treatment groups. $P < 0.05$ was considered statistically significant.

RESULTS

Evaluation of the nanoparticle's characteristics

The Cur/MgO NPs displayed absorbance at 266 nm attributable to the MgO nanoparticles, which are specific to MgO NPs and have a wavelength range between 260 and 280 nm (Fig. 3). Utilizing XRD pattern recognition, a confirmation analysis of the crystal structure was performed. XRD patterns were obtained by calcining the precursor at 500 °C. The particle size of the Cur/MgO NPs ($0.9\ \lambda/(\beta^*\cos\theta)$) was 160 to 165 nm using Debye Scherrer's formula (Fig. 4).

Employing the KBr pellet approach, FT-IR spectra in the solid phase were recorded between 400 and 4000 cm^{-1}. The sample underwent calcination at 500 °C for 4 h, and Fig. 5 depicts the

IR spectrum of Cur/MgO NPs. The broadband stretching vibration mode of the MgO moiety occurs between 438 and 769 cm^{-1}. The two distinct bands observed at the wave ranges of 1014 - 1074 cm^{-1} and 1590 -1641 cm^{-1} were attributed to the bending vibrations of the absorbed water molecules and the surface hydroxyl group (-OH), respectively. The OH stretching vibrations of the absorbed water molecule and the surface hydroxyl group caused a broad vibration band within the wave range of 3325-3553 cm^{-1}. The presence of an aromatic ring was confirmed by the band near 1387 cm^{-1}, caused by the C=C stretching frequency. The asymmetric stretching of the carbonate ion, CO_3^{2-} species, is attributed to the FT-IR absorption peak visible at 1501 cm^{-1}.

The morphology of the Cur/MgO NPs was studied using FE-SEM, which determined the average size of the NPs to be 164 nm with a modest amount of agglomeration (Fig. 6). The nanoparticles had a somewhat round shape.

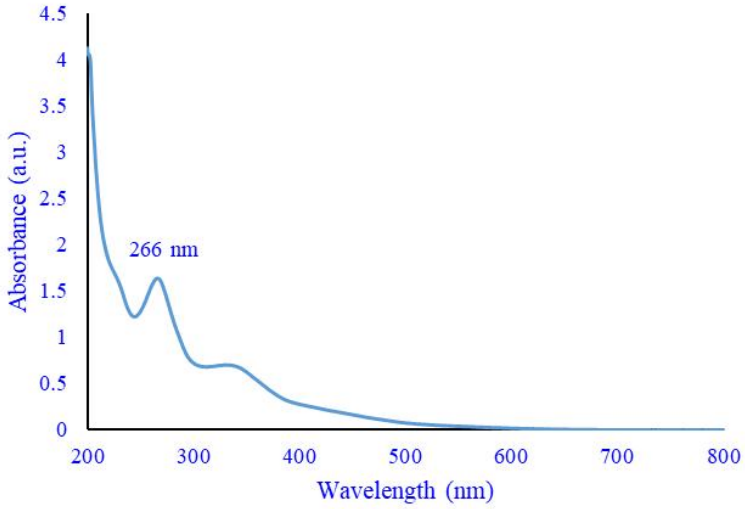

Fig. 3. UV spectra of curcumin/magnesium oxide nanoparticles.

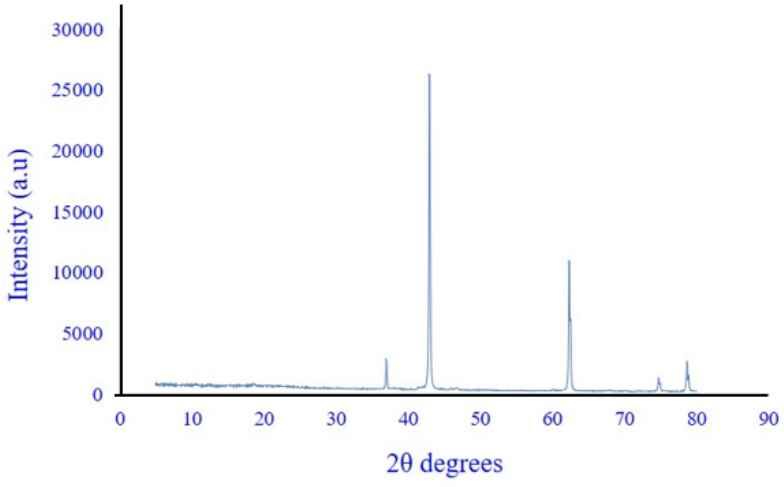

Fig. 4. X-ray diffractometer pattern of curcumin/magnesium oxide nanoparticles.

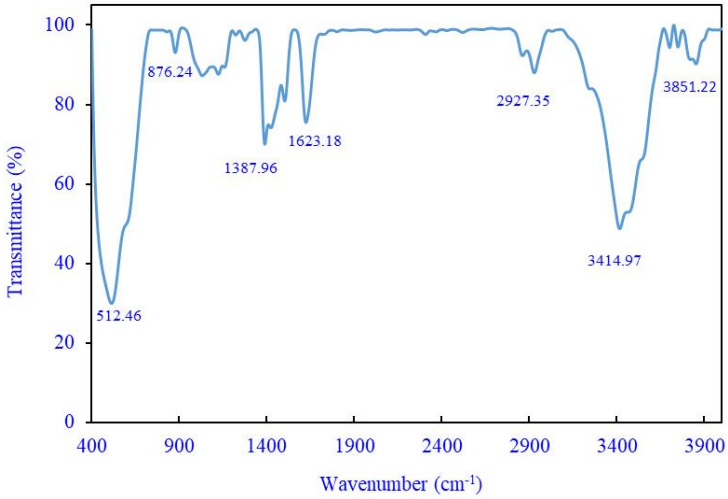

Fig. 5. Fourier transform infrared spectrum of curcumin/magnesium oxide nanoparticles.

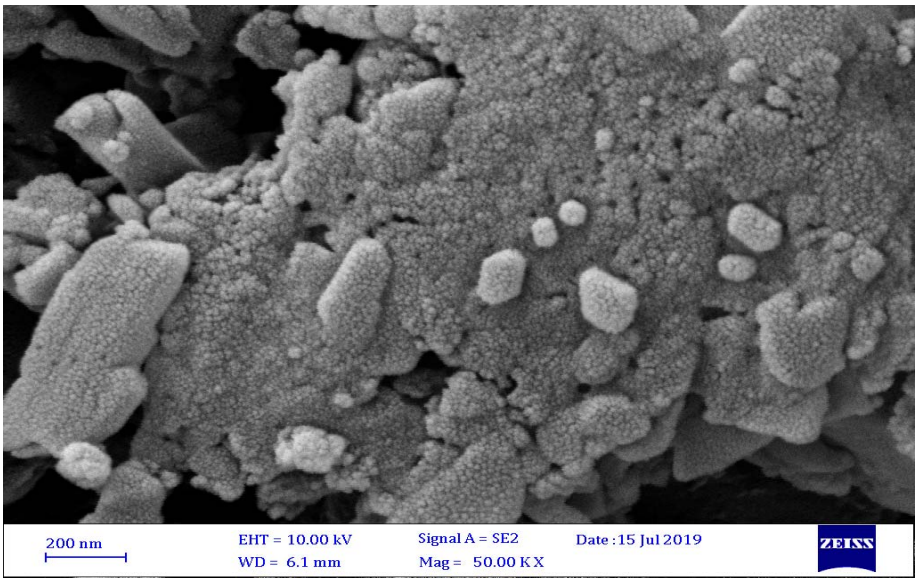

Fig. 6. Scanning electron microscopy image of curcumin/magnesium oxide nanoparticles.

In-vivo study

Effect of Cur/MgO NPs on ketamine-induced mitochondrial glutathione/glutathione disulfide

Ketamine (25 mg/kg) caused a significant reduction in GSH (F = 16.66) and a boost in GSSG (F = 5.44) levels compared to controls. In contrast, compared to mice treated with ketamine alone, the group treated with the ketamine-Cur combination (40 mg/kg) had elevated GSH (F = 16.66) levels and lower GSSG (F = 5.44) levels. Cur/MgO nanoparticles reversed the ketamine-induced decline in GSH (F = 16.66) and increased GSSG (F = 5.44). MgO (5 mg/kg) did not change the GSH and GGSG levels (Table 1).

Effect of Cur-MgO NPs on ketamine-induced oxidative stress

Ketamine decreased SOD (F = 18.47), GPx (F = 13.34), and GR (F = 21.13) activity compared to control mice while the levels of MDA (F = 8.561) were increased compared to control. The ketamine-Cur combination (40 mg/kg) induced the levels of SOD (F = 18.47), GPx (F = 13.34), and GR (F = 21.13) but lowered MDA levels (F = 8.56). When compared to mice that received ketamine, Cur/MgO NPs reversed the effect of ketamine-induced oxidative stress. MgO (5 mg/kg) did not change these oxidative stress parameters (Fig. 7 A-D).

Table 1. Effect of Cur/MgO NPs on mitochondrial GSH and GSSG content in ketamine-treated rats. Data are expressed as mean ± SEM, n = 7. $^{***}P < 0.001$ indicates significant differences compared to the control group and $^{###}P < 0.001$ versus the ketamine group.

Groups	GSH (nmol/mg protein)	GSSG (nmol/mg protein)	GSH/GSSG
Control	112.9 ± 8.6	0.82 ± 0.6	140
Ketamine (25 mg/kg)	21.4 ± 6.9***	19.1 ± 0.3***	1.1***
Ketamine + Cur (40 mg/kg)	90.2 ± 9.3$^{###}$	4.1 ± 0.5$^{###}$	21$^{###}$
Ketamine + Cur/MgO NPs (10 mg/kg)	79.6 ± 5.9$^{###}$	8.1 ± 0.4$^{###}$	9.8$^{###}$
Ketamine+ Cur/MgO NPs (20 mg/kg)	95.2 ± 8.2$^{###}$	4.2 ± 0.3$^{###}$	23$^{###}$
Ketamine+ Cur/MgO NPs 40 mg/kg)	110.6 ± 11.9$^{###}$	1.2 ± 0.1$^{###}$	91$^{###}$
MgO (5 mg/kg)	37.4 ± 8.9	10.3 ± 7.2***	3.7

Cur/MgO, Curcumin/magnesium oxide; NPs, nanoparticles; GSH, reduced form of glutathione; GSSG, oxidized form of glutathione.

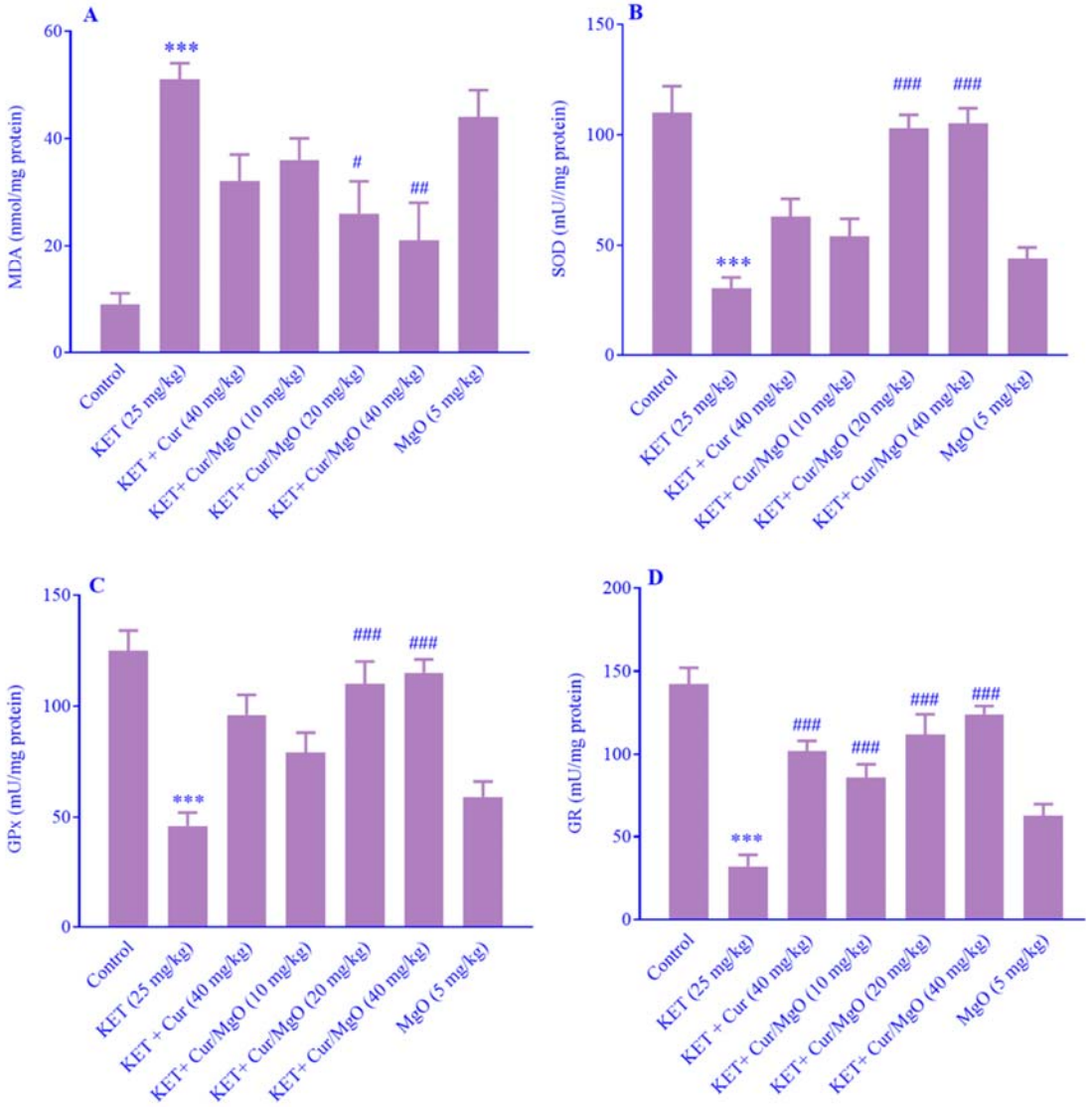

Fig. 7. Effects of Cur/MgO NPs on ketamine induced alteration in (A) lipid peroxidation, (B) SOD activity, (C) GPx activity, and (D) GR activity in rat isolated hippocampus. Data are expressed as mean ± SEM, n = 8. $^{***}P < 0.001$ indicates significant differences in comparison with the control; $^{#}P < 0.05$, $^{##}P < 0.01$, $^{###}P < 0.001$ versus ketamine (25 mg/kg). KET, Ketamine; Cur, curcumin; Cur/MgO NPs, curcumin/magnesium oxide nanoparticles; MDA, malondialdehyde; SOD, super oxide dismutase; GPx, glutathione peroxidase; GR, glutathione reductase.

Effect of Cur-MgO NPs on ketamine-induced inflammation

Compared to control mice, ketamine (25 mg/kg) significantly elevated both TNF-α (F = 6.94) and IL-1β (F = 8.56) levels. Ketamine plus Cur (40 mg/kg) lowered the levels of TNF-α (F = 6.94) and IL-1β (F = 8.56) compared to ketamine-treated mice. IL-1β (F = 8.56) and TNF-α (F = 6.94) were lower in those animals given the Cur/MgO NPs compared to KET alone, indicating the KET-induced inflammation was suppressed. MgO (5 mg/kg) did not change these inflammatory parameters (Fig. 8A and B).

Effect of Cur/MgO NPs on ketamine-induced apoptosis

Compared to controls, ketamine (25 mg/kg) significantly lowered Bcl-2 (F = 6.97) but significantly elevated Bax (F = 61.74), caspase-3 (F = 12.46), and caspase-7 (F = 12.36). Compared to ketamine treatment, mice receiving ketamine combined with Cur enhanced Bcl-2 (F = 6.97) levels and decreased Bax (F = 61.74), caspase-3 (F = 12.46), and caspase-7 (F = 12.36). Cur/MgO NPs significantly reduced the apoptotic effects of ketamine, as seen by a decrease in Bax (F = 61.74), caspase-3 (F = 12.46), and caspase-7 (F = 12.36) levels and a rise in Bcl-2 (F = 6.97) compared to ketamine-treated mice. MgO (5 mg/kg) did not change these apoptotic parameters (Fig. 9A-D).

Effect of Cur/MgO NPs on ketamine-induced mitochondrial chain enzyme

Compared to control mice, ketamine (25 mg/kg) significantly decreased the function of the mitochondrial complex I (F = 8.28), II (F = 11.40), III (F = 8.98), and IV (F = 5.13) enzymes. However, compared to the group that received merely ketamine, the mitochondrial complex I (F = 8.28), II (F = 11.40), III (F = 8.98), and IV (F = 5.13) enzymes increased in the groups treated with ketamine combined with Cur (40 mg/kg). Additionally, when compared to mice treated with ketamine, Cur/MgO NPs partially reversed the activity of the mitochondrial complex I (F = 8.28), II (F = 11.40), III (F = 8.98), and IV (F = 5.13) enzymes, suppressing ketamine-induced mitochondrial abnormalities. MgO (5 mg/kg) did not change the quadruple mitochondrial enzyme activities (Fig. 10A-D).

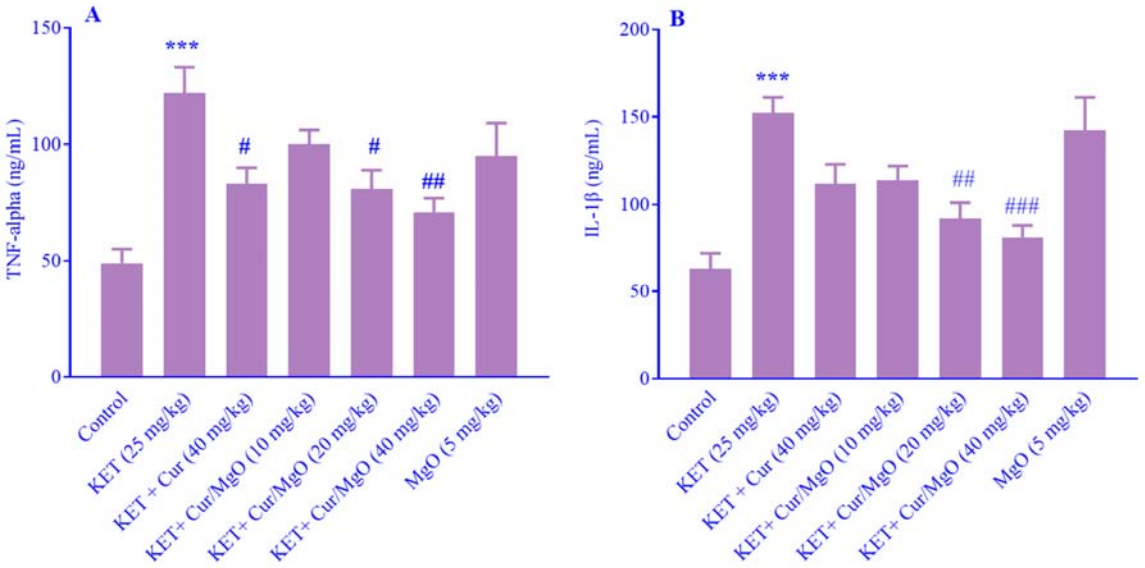

Fig. 8. Effects of Cur/MgO NPs on ketamine induced alteration in (A) TNF-α and (B) IL-1β level in rat isolated hippocampus. Data are expressed as mean ± SEM, n = 8. ***$P < 0.001$ indicates significant differences in comparison with the control; $^{\#}P < 0.05$, $^{\#\#}P < 0.01$, $^{\#\#\#}P < 0.001$ versus ketamine (25 mg/kg). KET, Ketamine; Cur, curcumin; Cur/MgO NPs, curcumin/magnesium oxide nanoparticles; TNF-α, tumor necrosis factor alpha; IL-1β, interleukin-1 beta.

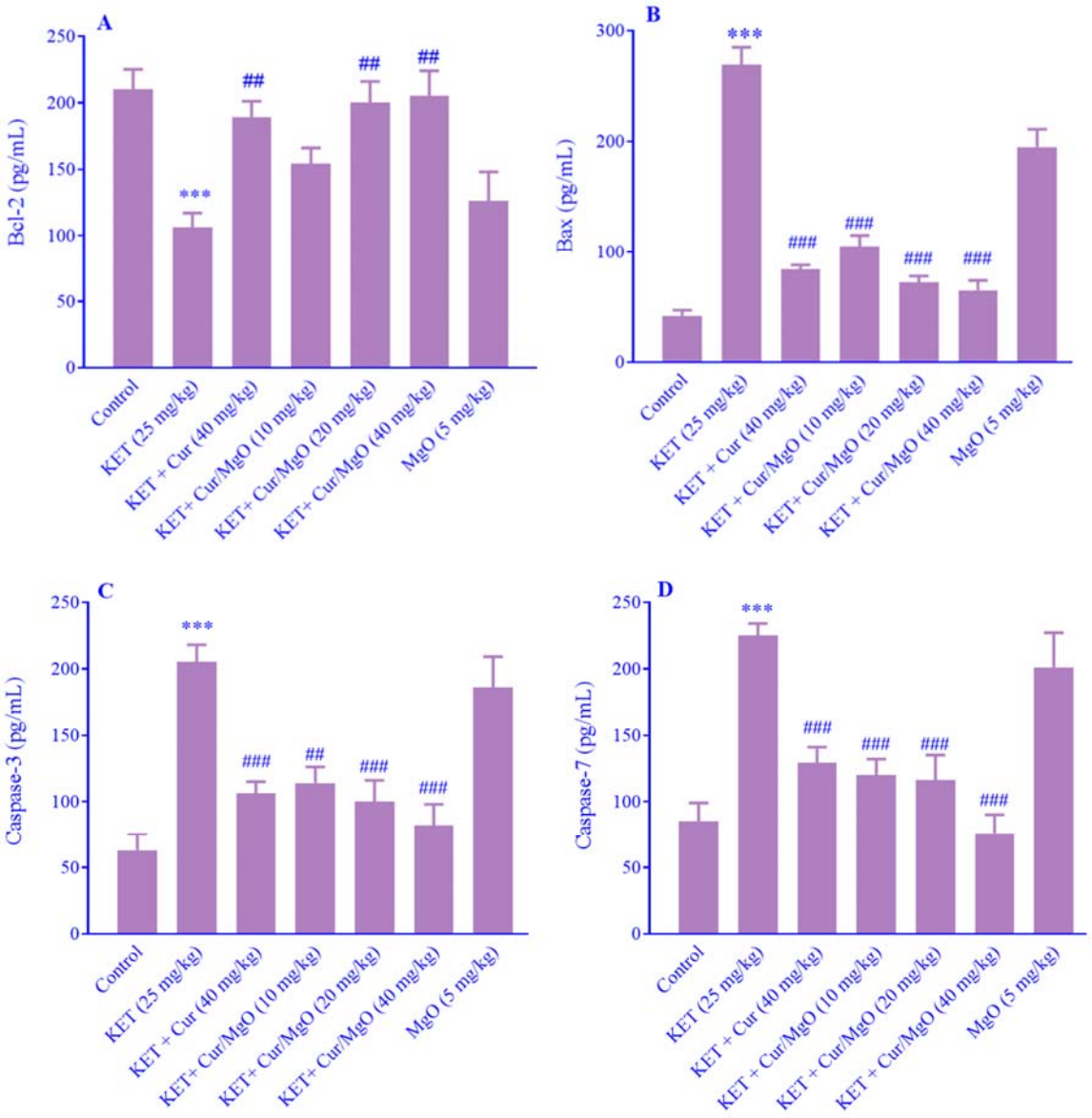

Fig. 9. Effects of Cur/MgO NPs on ketamine induced in protein expression of (A) Bax, (B) Bcl-2, (C) caspase-3, and (D) Caspase-7 in rat isolated hippocampus. Data are expressed as mean ± SEM, n = 8. ***$P < 0.001$ indicates significant differences in comparison with the control; $^{\#\#}P < 0.01$ and $^{\#\#\#}P < 0.001$ versus ketamine (25 mg/kg). KET, Ketamine; Cur, curcumin; Cur/MgO NPs, curcumin/magnesium oxide nanoparticles; Bcl2, B-cell lymphoma 2; Bax, Bcl-2 Associated X-protein.

Effect of Cur/MgO NPs on ketamine-induced histopathology

Ketamine (25 mg/kg) significantly reduced both granular cells in the dentate gyrus (DG) areas (F = 9.58) and pyramidal cells in the cornu ammonis area 1 (CA1; F = 9.83) areas of the hippocampus (Table 2). Cell shrinkage and degeneration (Figs. 11 and 12) were observed in both regions. Both ketamine + Cur and ketamine + Cur/MgO NPs increased the number of granular cells in the DG (F = 9.58) and pyramidal cells in the CA1 (F = 9.83) area of the hippocampus. MgO alone did not affect these histological observations (Table 2, Figs. 11 and 12).

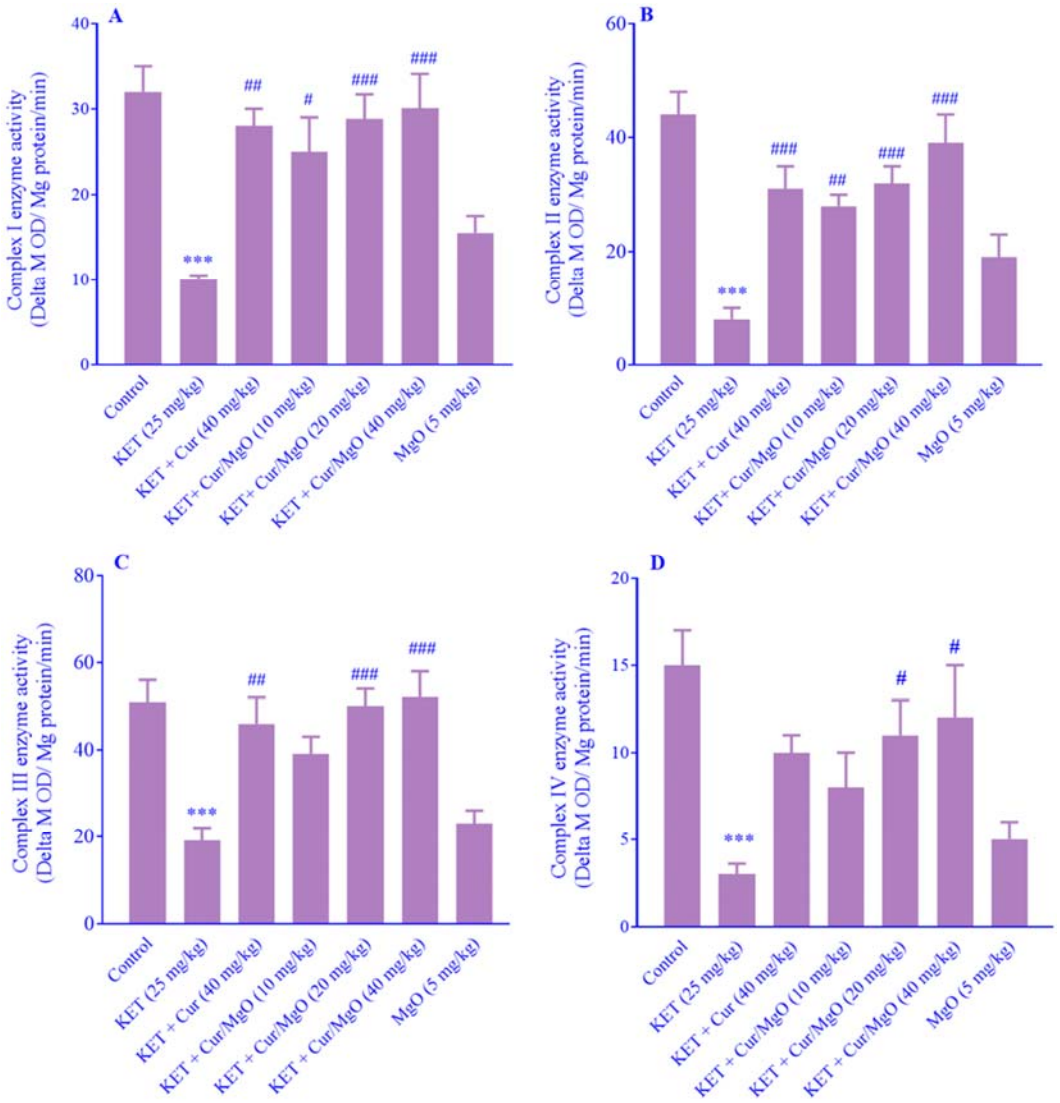

Fig. 10. Effects of Cur/MgO NPs on ketamine induced mitochondrial complex enzymes activity, (A) complex I, (B) complex II, (C) complex III, (D) and complex III in rat isolated hippocampus. Data are expressed as mean ± SEM, n = 8. ***$P < 0.001$ indicates significant differences in comparison with the control; $^{\#}P < 0.05$, $^{\#\#}P < 0.01$, and $^{\#\#\#}P < 0.001$ versus ketamine (25 mg/kg). KET, Ketamine; Cur, curcumin; Cur/MgO NPs, curcumin/magnesium oxide nanoparticles.

Table 2. Effects of Cur/MgO NPs on hippocampus neuronal granular cells of DG area and pyramidal cells of CA1 area, counting (number/mm) in ketamine-treated rats. Data are expressed as mean ± SEM, n = 7. $^{***}P < 0.001$ indicates significant differences compared to the control group and $^{\#}P < 0.05$ versus the ketamine group and $^{\#\#\#}P < 0.001$ versus the ketamine group.

Groups	Number of cells in DG (number/mm)	Number of cells in CA1(number/mm)
Control group	325.1 ± 28	217 ± 12
Ketamine (25 mg/kg)	112 ± 14***	81 ± 8***
Ketamine + Cur (40 mg/kg)	310 ± 33$^{\#\#\#}$	202 ± 11$^{\#\#\#}$
Ketamine+ Cur/MgO NPs (10 mg/kg)	156 ± 18	105 ± 9
Ketamine+ Cur/MgO NPs (20 mg/kg)	289 ± 31$^{\#\#\#}$	173 ± 14$^{\#\#\#}$
Ketamine+ Cur/MgO NPs 40 mg/kg)	318 ± 29$^{\#\#\#}$	212 ± 15$^{\#\#\#}$
MgO (5 mg/kg)	298 ± 36	198 ± 15

Cur/MgO, Curcumin/magnesium oxide; NPs, nanoparticles; GSH, reduced form of glutathione; GSSG, oxidized form of glutathione; DG, dentate gyrus; CA1, cornu ammonis area 1.

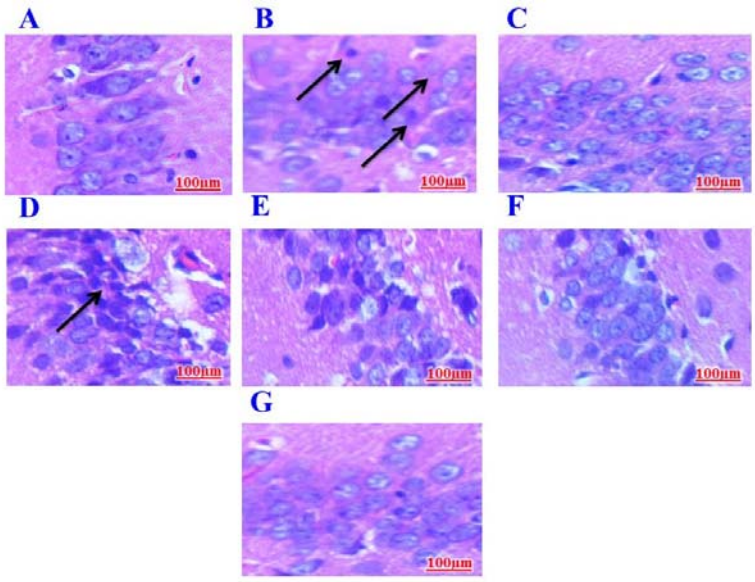

Fig. 11. Representative images of hematoxylin and eosin-stained granular cells of the DG area of the left hippocampus. (A) Control group, (B) ketamine (25 mg/kg), (C) ketamine (25 mg/kg) and Cur (40 mg/kg), (D-F) ketamine (25 mg/kg) and Cur-MgO NPs (10, 20, or 40 mg/kg, and (G) ketamine (25 mg/kg) and MgO (5 mg/kg). Black arrows indicate the vacuolation and neuronal degeneration in the DG area of the mouse hippocampus. Magnification × 400. Cur, curcumin; Cur/MgO NPs, curcumin/magnesium oxide nanoparticles; DG, dentate gyrus.

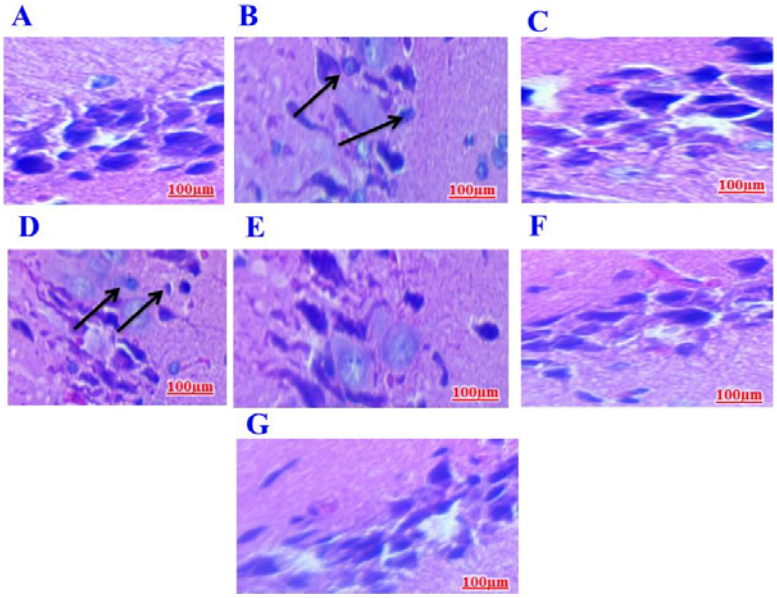

Fig. 12. Representative images of hematoxylin and eosin-stained pyramidal cells of the CA1 area. (A) Control group, (B) ketamine (25 mg/kg), (C) ketamine (25 mg/kg) and Cur (40 mg/kg), (D-F) ketamine (25 mg/kg) and Cur-MgO NPs (10, 20, or 40 mg/kg, and (G) ketamine (25 mg/kg) and MgO (5 mg/kg). Black arrows indicate the vacuolation and neuronal degeneration in the DG area of the mouse hippocampus. Magnification × 400. Cur, curcumin; Cur/MgO NPs, curcumin/magnesium oxide nanoparticles; CA1, cornu ammonis area 1.

DISCUSSION

Ketamine, an NMDA receptor antagonist (3) and schedule 3 drug (https://www.dea.gov/drug-information/drug-scheduling), causes neuro-degeneration accompanied by apoptosis, oxidative stress, inflammation, histological changes, and decreased mitochondrial respiratory chain enzyme activity. According to several recent studies (21,50,51), ketamine caused neuronal cell death and

neurodegeneration in the developing rat brain, but the mechanism behind these pathological alterations was not characterized. In obstetric and pediatric patients, ketamine is frequently used for anesthesia and analgesia (19,21,52), even though it has a high-risk profile for producing hallucinations and delusions (53) and is often abused (26).

Several studies have noted Cur's potential oxidant-antioxidant modification in drug users (37,54). The antioxidative characteristics of Cur have been verified by *in vivo* and *in vitro* experiments. Cur confers its neuroprotection against oxidative stress by affecting the genes and proteins involved in oxidative stress (55,56). Cur lowered the increase in TNF-α, IL-1β, and TGF-β1 levels in mouse-rat hybrid retina ganglion cells and in rats postnatally exposed to ethanol (57-59). However, these experiments did not assess the antioxidative effects of metal complexed nanoparticles such as Cur/MgO NPs (54).

Cur-loaded metal oxide nanoparticles, specifically Cur/MgO NPs (60) enhanced the biocompatibility of Cur in mice and rats (61,62). These studies, which considered the possibilities of Cur bonding with metal oxides, also suggested that these nanoparticles do not rapidly degrade under *in vivo* conditions.

Hippocampal cells are susceptible to ketamine (63-66). Ketamine caused a persistent stress reaction, which caused changes in hippocampal AMPA receptors and cognitive impairments in chronic ketamine addiction models (66,67). Ketamine lowered neuronal cell survival rates in a time- and dose-dependent way in human neurons differentiated from embryonic stem cells *via* the mitochondrial apoptosis pathway (68,69). Oxidative stress and decreased antioxidant levels in the rodent brain have been linked to ketamine-induced toxicity (63,70). Hydroxyl radicals, such as reactive oxygen species (ROS), are formed during oxidative stress and can induce DNA oxidation, resulting in errors and DNA replication mutations (68,71). Ketamine enhanced the production of ROS, which, in turn, caused inflammation in human neural stem cells. DNA damage and cellular death may follow (71).

There are limited studies on managing ketamine toxicity. Cur, the principal curcuminoid in turmeric, is neuroprotective and has antioxidant, anti-inflammatory, and anti-apoptosis properties (37,72-75). Cur has been reported to confer neuroprotection, partly through scavenging free radicals. Since Cur is also known for its immunomodulatory properties and activity against oxidation, inflammation, and apoptosis (76). It may have therapeutic promise for neurodegenerative diseases, such as Alzheimer's disease and Parkinson's disease (37,77-79). Further, by lowering lipid peroxidation and boosting the function of antioxidant enzymes such as SOD, catalase, and GSH-related antioxidants, Cur may combat oxidative stress (80,81). Cur, however, has limited bioavailability. Nanotechnology has been reported to increase the bioavailability of Cur and reduce its toxicity. Targeted delivery, as the Cur-MgO NP, should improve the effectiveness of Cur (82,83).

In the current study, we evaluated Cur-MgO NPs against ketamine-induced neurotoxicity in mouse hippocampal cells by evaluating morphological, mitochondrial function, anti-inflammatory, antioxidant, and anti-apoptotic changes. Ketamine boosted IL-1β, TNF-α, and Bax levels while decreasing Bcl-2 levels and increased lipid peroxidation and GSSG while decreasing GSH and several antioxidant enzymes such as GPx, GR, and SOD. Cur and the Cur/MgO NPs counteracted these ketamine-induced neurodegenerative alterations. The ketamine-induced reduction of the mitochondrial complexes I, II, III, and IV respiratory chain enzymes was also reversed by Cur/MgO NPs. Cur/MgO NPs and Cur also reduced ketamine-induced changes in the hippocampus's CA1 and DG cell morphology and cell count. Both prevented increased MDA levels in the ketamine-treated group, thereby reducing lipid peroxidation. Cur/MgO NPs were more effective than Cur.

Our conclusions align with earlier research that showed increased pro-inflammatory cytokines and apoptosis after persistent ketamine use or abuse (63-65) and that Cur can prevent apoptosis and neuro-inflammation caused by ketamine (37,54). The role of Cur as an anti-inflammatory and anti-apoptotic agent has been reported in numerous studies (37,72-75,84,85). Curcumin exerts its anti-inflammatory property by inhibiting several inflammatory pathways, such as the cytokines and chemokines pathways, the cyclooxygenase-prostaglandin, nitric oxide synthase-nitric oxide, nuclear factor kappa B, JAK/STAT, Toll-like receptors, and mitogen-activated protein kinase signaling pathways (37,72-75,84,85).

We have speculated that the neuroprotective effect of Cur and Cur/MgO NPs is probably caused by the activation of the genes and proteins involved

in the biogenesis of the mitochondria and their respiratory chain (86,87). Since the Cur/MgO NP was more effective than Cur, the Cur/MgO NPs may be a better candidate for evaluation as a potential drug in cases of KET abuse (88,89).

CONCLUSION

We successfully synthesized a Cur-conjugated MgO nanoparticle (Fig. 4). Both Cur and Cur/MgO NPs inhibited the ketamine-induced neurotoxicity in the mouse hippocampus by reversing mitochondrial dysfunction, oxidative stress, inflammation, apoptosis, and histomorphological changes induced by ketamine. Cur/MgO NPs were more effective than Cur in reversing ketamine-induced neurotoxicity.

Limitations

This study investigated limited doses of Cur/MgO NPs for a relatively short exposure in male mice treated with a single dose of ketamine. Further, only limited parameters related to cell degeneration and death were examined. In addition to efficacy studies in humans, the potential side effects of the Cur/MgO NPs need further investigation, both at the bench and in clinical trials.

Acknowledgments

We sincerely thank the Department of Pharmaceutical Chemistry, Faculty of Pharmaceutical Chemistry, Tehran Medical Sciences, Islamic Azad University, Tehran, Iran, for their technical support of this work and for helping synthesize nanoparticles. This study was the continuation of the M.Sc. thesis project at the Islamic Azad University, Tehran, Iran, whose ethical code is IR.IAU.PS.REC.1398.353. Current projects were financially supported by Masih Daneshvari Hospital, which is affiliated with Shahid Beheshti University of Medical Sciences, Tehran, Iran, and its ethical code is I.R.SBMU.NRITLD.REC.1402.093.

Conflict of interest statements

All authors confirmed no conflict of interest in this study.

Authors' contributions

M. Motaghinejad contributed to the conception and design of the study. Data acquisition and analysis were carried out by M. Salehirad, while data interpretation was performed by A. Wallace Hayes and M. Gholami. All manuscript drafts were critically reviewed and revised by M. Motaghinejad and A. Wallace Hayes. The final version of the article was read and approved by all authors.

REFERENCES

1. Couvreur P. Nanoparticles in drug delivery: past, present and future. Adv Drug Deliv Rev. 2013;65(1):21-23. DOI: 10.1016/j.addr.2012.04.010.
2. Freitas Jr RA. What is nanomedicine?Nanomedicine.2005;1(1):2-9. DOI: 10.1016/j.nano.2004.11.003.
3. Kesmati M, Konani M, Torabi M, Khajehpour L. Magnesium oxide nanoparticles reduce anxiety induced by morphine withdrawal in adult male mice. Physiol Pharmacol. 2016;20(3):197-205.
4. Mahmoud A, Ezgi Ö, Merve A, Özhan G. *In vitro* toxicological assessment of magnesium oxide nanoparticle exposure in several mammalian cell types. Int J Toxicol. 2016;35(4):429-437. DOI: 10.1177/1091581816648624.
5. Kesmati M, Sargholi Notarki Z, Issapareh N, Torabi M. Comparison the effect of zinc oxide and magnesium oxide nano particles on long term memory in adult male mice. Zahedan J Res Med Sci. 2016;18:e3473,1-6. DOI: 10.17795/zjrms-3473.
6. Jahangiri L, Kesmati M, Najafzadeh H. Evaluation of analgesic and anti-inflammatory effect of nanoparticles of magnesium oxide in mice with and without ketamine. Eur Rev Med Pharmacol Sci. 2013;17(20):2706-2710. PMID: 24174350.
7. Moeini-Nodeh S, Rahimifard M, Baeeri M, Abdollahi M. Functional improvement in rats' pancreatic islets using magnesium oxide nanoparticles through antiapoptotic and antioxidant pathways. Biol Trace Elem Res. 2017;175(1):146-155. DOI: 10.1007/s12011-016-0754-8.
8. Gazal M, Valente MR, Acosta BA, Kaufmann FN, Braganhol E, Lencina CL, *et al*. Neuroprotective and antioxidant effects of curcumin in a ketamine-induced model of mania in rats. Eur J Pharmacol. 2014;724:132-139. DOI: 10.1016/j.ejphar.2013.12.028.
9. Zhang X, Cui Y, Song X, Jin X, Sheng X, Xu X, *et al*. Curcumin alleviates ketamine-induced oxidative stress and apoptosis via Nrf2 signaling pathway in rats' cerebral cortex and hippocampus. Environ Toxicol. 2023;38(2):300-311. DOI: 10.1002/tox.23697.
10. Mohammadi M, Abadi FS, Haddadi R, Nili-Ahmadabadi A. Antinociceptive and anti-inflammatory actions of curcumin and nano curcumin:a comparative study. Res Pharm Sci. 2023;18(6):604-613. DOI: 10.4103/1735-5362.389948.

11. Zamani E, Klour RA, Shekarsarayi AG, Ghazizadeh F, Evazalipour M. *In vitro* and *in vivo* assessment of indomethacin-induced genotoxicity: protection by curcumin. Res Pharm Sci. 2024;19(2):178-187. DOI: 10.4103/RPS.RPS_100_23.
12. Mobinhosseini F, Salehirad M, Wallace Hayes A, Motaghinejad M, Hekmati M, Safari S, *et al*. Curcumin-ZnO conjugated nanoparticles confer neuroprotection against ketamine-induced neurotoxicity. J Biochem Mol Toxicol. 2024;38(1):e23611. DOI: 10.1002/jbt.23611.
13. Shome S, Talukdar AD, Choudhury MD, Bhattacharya MK, Upadhyaya H. Curcumin as potential therapeutic natural product:a nanobiotechnological perspective. J Pharm Pharmacol. 2016;68(12):1481-1500. DOI: 10.1111/jphp.12611.
14. Sudakaran SV, Venugopal JR, Vijayakumar GP, Abisegapriyan S, Grace AN, Ramakrishna S. Sequel of MgO nanoparticles in PLACL nanofibers for anti-cancer therapy in synergy with curcumin/β-cyclodextrin. Mater Sci Eng C Mater Biol Appl. 2017;71:620-628. DOI: 10.1016/j.msec.2016.10.050.
15. Brietzke E, Mansur RB, Zugman A, Carvalho AF, Macêdo DS, Cha DS, *et al*. Is there a role for curcumin in the treatment of bipolar disorder?. Med Hypotheses. 2013;80(5):606-612. DOI: 10.1016/j.mehy.2013.02.001.
16. Kandhare AD, Raygude KS, Ghosh P, Ghule AE, Bodhankar SL. Therapeutic role of curcumin in prevention of biochemical and behavioral aberration induced by alcoholic neuropathy in laboratory animals. Neurosci Lett. 2012;511(1):18-22. DOI: 10.1016/j.neulet.2012.01.019.
17. Stohs SJ, Chen O, Ray SD, Ji J, Bucci LR, Preuss HG. Highly bioavailable forms of curcumin and promising avenues for curcumin-based research and application:a review. Molecules. 2020;25(6):1397,1-12. DOI: 10.3390/molecules25061397.
18. Das MK, Chakraborty T. Curcumin nano-theraputics for cancer chemotherapy: promises and challenges for the future. Eur J Pharm Med Res. 2016;3(3):177-1791.
19. Liu F, G Paule M, Ali S, Wang C. Ketamine-induced neurotoxicity and changes in gene expression in the developing rat brain. Curr Neuropharmacol. 2011;9(1):256-261. DOI: 10.2174/157015911795017155.
20. Cao Se, Tian J, Chen S, Zhang X, Zhang Y. Role of miR-34c in ketamine-induced neurotoxicity in neonatal mice hippocampus. Cell Biol Int. 2015;39(2):164-168. DOI: 10.1002/cbin.10349.
21. Jiang S, Li X, Jin W, Duan X, Bo L, Wu J, *et al*. Ketamine-induced neurotoxicity blocked by N-Methyl-d-aspartate is mediated through activation of PKC/ERK pathway in developing hippocampal neurons. Neurosci Lett. 2018;673:122-131. DOI: 10.1016/j.neulet.2018.02.051.
22. Eneni A-EO, Ben-Azu B, Ajayi AM, Aderibibge AO. Lipopolysaccharide exacerbates ketamine-induced psychotic-like behavior, oxidative stress, and neuroinflammation in mice: ameliorative effect of diosmin. J Mol Neurosci. 2023;73(2):129-142. DOI: 10.1007/s12031-022-02077-9.
23. Ommati MM, Mobasheri A, Niknahad H, Rezaei M, Alidaee S, Arjmand A, *et al*. Low-dose ketamine improves animals' locomotor activity and decreases brain oxidative stress and inflammation in ammonia-induced neurotoxicity. J Biochem Mol Toxicol. 2023;37(11):e23468,1-10. DOI: 10.1002/jbt.23468.
24. Oshodi TO, Ben-Azu B, Ishola IO, Ajayi AM, Emokpae O, Umukoro S. Molecular mechanisms involved in the prevention and reversal of ketamine-induced schizophrenia-like behavior by rutin: the role of glutamic acid decarboxylase isoform-67, cholinergic, Nox-2-oxidative stress pathways in mice. Mol Biol Rep. 2021;48(3):2335-2350. DOI: 10.1007/s11033-021-06264-6.
25. Sassano-Higgins S, Baron D, Juarez G, Esmaili N, Gold M. A review of ketamine abuse and diversion. Depress Anxiety. 2016;33(8):718-727. DOI: 10.1002/da.22536.
26. Bokor G, Anderson PD. Ketamine:an update on its abuse. J Pharm Pract. 2014;27(6):582-586. DOI: 10.1177/0897190014525754.
27. Lundberg M, Curbo S, Bohman H, Agartz I, Ögren SO, Patrone C, *et al*. Clozapine protects adult neural stem cells from ketamine-induced cell death in correlation with decreased apoptosis and autophagy. Biosci Rep. 2020;40(1):1-11. DOI: 10.1042/BSR20193156.
28. Venkataramaiah C, Priya BL, Payani S, Pradeepkiran JA. Pharmacological potentiality of bioactive flavonoid against ketamine induced cell death of PC 12 cell lines:an *in vitro* study. Antioxidants (Basel). 2021;10(6):934,1-17. DOI: 10.3390/antiox10060934.
29. Adibipour F, Salehirad M, Hayes AW, Hekmati M, Motaghinejad M. Preventive effect of ZnO-metformin nanocomposite against carbon tetrachloride-induced hepatotoxicity. Nanomed Res J. 2024;9(2):155-163. DOI: 10.22034/nmrj.2024.02.004.
30. Tohamy HG, El Okle OS, Goma AA, Abdel-Daim MM, Shukry M. Hepatorenal protective effect of nano-curcumin against nano-copper oxide-mediated toxicity in rats: Behavioral performance, antioxidant, anti-inflammatory, apoptosis, and histopathology. Life Sci. 2022; 292:120296. DOI: 10.1016/j.lfs.2021.120296.
31. Hettiarachchi SS, Dunuweera SP, Dunuweera AN, Rajapakse RMG. Synthesis of curcumin nanoparticles from raw turmeric rhizome. ACS Omega, 2021;**6**(12):8246-8252. DOI:10.1021/acsomega.0c06314.
32. Kilkenny C, Browne W, Cuthill IC, Emerson M, Altman DG. Animal research: reporting in vivo

experiments: the ARRIVE guidelines. Br J Pharmacol. 2010;160(7):1577-1579. DOI: 10.1111/j.1476-5381.2010.00872.x.
33. Shehata YM, Mansour M, Shadad S, Arisha A. Effect of curcumin-magnesium oxide nanoparticles conjugate in type-II diabetic rats. Adv Anim Vet Sci. 2020;8(s1):26-33. DOI:10.17582/journal.aavs/2020/8.s1.26.33.
34. Bose U, Broadbent JA, Juhász A, Karnaneedi S, Johnston EB, Stockwell S, *et al*. Protein extraction protocols for optimal proteome measurement and arginine kinase quantitation from cricket Acheta domesticus for food safety assessment. Food Chem. 2021;348:129110,1-11. DOI: 10.1016/j.foodchem.2021.129110.
35. Fernández-Vizarra E, Fernández-Silva P, Enríquez JA. Isolation of mitochondria from mammalian tissues and cultured cells. Cell Biol. 2006;2:69-77. DOI:10.1016/B978-012164730-8/50082-4.
36. Kruger NJ. The Bradford method for protein quantitation.Methods Mol Biol. 1994;32:9-15. DOI: 10.1385/0-89603-268-X:9.
37. Motaghinejad M, Motevalian M, Fatima S, Hashemi H, Gholami M. Curcumin confers neuroprotection against alcohol-induced hippocampal neurodegeneration via CREB-BDNF pathway in rats. Biomed Pharmacother. 2017;87:721-740. DOI: 10.1016/j.biopha.2016.12.020.
38. Motaghinejad M, Seyedjavadein Z, Motevalian M, Asadi M. The neuroprotective effect of lithium against high dose methylphenidate:possible role of BDNF. Neurotoxicology. 2016;56:40-54. DOI: 10.1016/j.neuro.2016.06.010.
39. Motaghinejad M, Karimian SM, Motaghinejad O, Shabab B, Asadighaleni M, Fatima S. The effect of various morphine weaning regimens on the sequelae of opioid tolerance involving physical dependency, anxiety and hippocampus cell neurodegeneration in rats. Fundam Clin Pharmacol. 2015;29(3):299-309. DOI: 10.1111/fcp.12121.
40. Motaghinejad M, Motevalian M, Fatima S. Mediatory role of NMDA, AMPA/kainate, GABAA and Alpha2 receptors in topiramate neuroprotective effects against methylphenidate induced neurotoxicity in rat. Life Sci. 2017;179:37-53. DOI: 10.1016/j.lfs.2017.01.002.
41. Motaghinejad M, Motevalian M, Fatima S, Beiranvand T, Mozaffari S. Topiramate via NMDA, AMPA/kainate, GABAA and Alpha2 receptors and by modulation of CREB/BDNF and Akt/GSK3 signaling pathway exerts neuroprotective effects against methylphenidate-induced neurotoxicity in rats. J Neural Transm (Vienna). 2017;124(11):1369-1387. DOI: 10.1007/s00702-017-1771-2.
42. Motaghinejad M, Motevalian M, Falak R, Heidari M, Sharzad M, Kalantari E. Neuroprotective effects of various doses of topiramate against methylphenidate-induced oxidative stress and inflammation in isolated rat amygdala:the possible role of CREB/BDNF signaling pathway. J Neural Transm (Vienna). 2016;123(12):1463-1477. DOI: 10.1007/s00702-016-1619-1.
43. Gholami M, Ghelichkhani Z, Aghakhani R, Klionsky DJ, Motaghinejad O, Motaghinejad M, *et al*. Minocycline acts as a neuroprotective agent against tramadol-induced neurodegeneration:behavioral and molecular evidence. Int J Prev Med. 2024;15:47,1-21. DOI: 10.4103/ijpvm.ijpvm_10_24.
44. Al Seyedan A, Dezfoulian O, Alirezaei M. *Satureja khuzistanica Jamzad* essential oil prevents doxorubicin-induced apoptosis via extrinsic and intrinsic mitochondrial pathways. Res Pharm Sci. 2020;15(5):481-490. DOI: 10.4103/1735-5362.297851.
45. Kirby DM, Thorburn DR, Turnbull DM, Taylor RW. Biochemical assays of respiratory chain complex activity. Methods Cell Biol. 2007;80:93-119. DOI: 10.1016/S0091-679X(06)80004-X.
46. Bénit P, Goncalves S, Dassa EP, Brière JJ, Martin G, Rustin P. Three spectrophotometric assays for the measurement of the five respiratory chain complexes in minuscule biological samples. Clin Chim Acta. 2006;374(1-2):81-86. DOI: 10.1016/j.cca.2006.05.034.
47. Kim Suvarna S, Layton Ch, Bancroft JD. Bancroft's Theory and Practice of Histological Techniques. In: Bancroft JD, Layton C. The hematoxylins and eosin. Bancroft's theory and practice of histological techniques. Elsevier; 2012. pp. 126-138. DOI: 10.1016/C2015-0-00143-5.
48. Cardiff RD, Miller CH, Munn RJ. Manual hematoxylin and eosin staining of mouse tissue sections. Cold Spring Harb Protoc. 2014;2014(6):655-658. DOI: 10.1101/pdb.prot073411.
49. Sahay A, Hen R. Adult hippocampal neurogenesis in depression. Nat Neurosci. 2007;10(9):1110-1115. DOI: 10.1038/nn1969.
50. Zheng X, Zhou J, Xia Y. The role of TNF-α in regulating ketamine-induced hippocampal neurotoxicity. Arch Med Sci. 2015;11(6):1296-1302. DOI: 10.5114/aoms.2015.56355.
51. Huang L, Liu Y, Jin W, Ji X, Dong Z. Ketamine potentiates hippocampal neurodegeneration and persistent learning and memory impairment through the PKCγ-ERK signaling pathway in the developing brain. Brain Res. 2012;1476:164-171. DOI: 10.1016/j.brainres.2012.07.059.
52. Jørum E, Warncke T, Stubhaug A. Cold allodynia and hyperalgesia in neuropathic pain: the effect of N-methyl-D-aspartate (NMDA) receptor antagonist ketamine–a double-blind, cross-over comparison with alfentanil and placebo. Pain. 2003;101(3):229-235. DOI: 10.1016/S0304-3959(02)00122-7.
53. Powers III AR, Gancsos MG, Finn ES, Morgan PT, Corlett PR. Ketamine-induced hallucinations. Psychopathology. 2015;48(6):376-385. DOI: 10.1159/000438675.
54. Menon VP, Sudheer AR. Antioxidant and anti-inflammatory properties of curcumin. Adv Exp Med Biol. 2007;595:105-125. DOI: 10.1007/978-0-387-46401-5_3.

55. Scapagnini G, Colombrita C, Amadio M, D'Agata V, Arcelli E, Sapienza M, *et al*. Curcumin activates defensive genes and protects neurons against oxidative stress. Antioxid Redox Signal. 2006;8(3-4):395-403.
DOI: 10.1089/ars.2006.8.395.
56. Shishodia S. Molecular mechanisms of curcumin action: gene expression. Biofactors. 2013;39(1):37-55.
DOI: 10.1002/biof.1041.
57. Perez-Torres I, Ruiz-Ramirez A, Banos G, El-Hafidi M. *Hibiscus Sabdariffa Linnaeus* (Malvaceae), curcumin and resveratrol as alternative medicinal agents against metabolic syndrome. Cardiovasc Hematol Agents Med Chem. 2013;11(1):25-37.
DOI: 10.2174/1871525711311010006.
58. Tiwari V, Chopra K. Attenuation of oxidative stress, neuroinflammation, and apoptosis by curcumin prevents cognitive deficits in rats postnatally exposed to ethanol. Psychopharmacology (Berl). 2012;224(4):519-535.
DOI: 10.1007/s00213-012-2779-9.
59. Lu HF, Yang JS, Lai KC, Hsu SC, Hsueh SC, Chen YL, *et al*. Curcumin-induced DNA damage and inhibited DNA repair genes expressions in mouse–rat hybrid retina ganglion cells (N18). Neurochem Res. 2009;34(8):1491-1497.
DOI: 10.1007/s11064-009-9936-5.
60. Shehata Y, Mansour M, Shadad S, Metwally M, Arisha A. Anti-diabetic effects of curcumin-magnesium oxide nanoparticles conjugate in type 2 diabetic rats. Zagazig Vet J. 2020;48(3):263-272.
DOI: 10.21608/zvjz.2020.23007.1098.
61. Prasad S, DuBourdieu D, Srivastava A, Kumar P, Lall R. Metal–curcumin complexes in therapeutics: an approach to enhance pharmacological effects of curcumin. Int J Mol Sci. 2021;22(13):7094,1-24.
DOI: 10.3390/ijms22137094.
62. Beyene AM, Moniruzzaman M, Karthikeyan A, Min T. Curcumin nanoformulations with metal oxide nanomaterials for biomedical applications. Nanomaterials (Basel). 2021;11(2):460,1-22.
DOI: 10.3390/nano11020460.
63. Onaolapo A, Ayeni O, Ogundeji M, Ajao A, Onaolapo O, Owolabi A. Subchronic ketamine alters behaviour, metabolic indices and brain morphology in adolescent rats: involvement of oxidative stress, glutamate toxicity and caspase-3-mediated apoptosis. J Chem Neuroanat. 2019;96:22-33.
DOI: 10.1016/j.jchemneu.2018.12.002.
64. Li Y, Shen R, Wen G, Ding R, Du A, Zhou J, *et al*. Effects of ketamine on levels of inflammatory cytokines IL-6, IL-1β, and TNF-α in the hippocampus of mice following acute or chronic administration. Front Pharmacol. 2017;8:139,1-14.
DOI: 10.3389/fphar.2017.00139.
65. Sun L, Li Q, Li Q, Zhang Y, Liu D, Jiang H, *et al*. Chronic ketamine exposure induces permanent impairment of brain functions in adolescent cynomolgus monkeys. Addict Biol. 2014;19(2):185-194.
DOI: 10.1111/adb.12004.
66. Ding R, Li Y, Du A, Yu H, He B, Shen R, *et al*. Changes in hippocampal AMPA receptors and cognitive impairments in chronic ketamine addiction models:another understanding of ketamine CNS toxicity. Sci Rep. 2016;6:38771,1-11.
DOI: 10.1038/srep38771.
67. Sinner B, Friedrich O, Zink W, Zausig Y, Graf BM. The toxic effects of s (+)-ketamine on differentiating neurons *in vitro* as a consequence of suppressed neuronal Ca2+ oscillations. Anesth Analg. 2011;113(5):1161-1169.
DOI: 10.1213/ANE.0b013e31822747df.
68. J Bosnjak Z, Yan Y, Canfield S, Y Muravyeva M, Kikuchi C, W Wells C, *et al*. Ketamine induces toxicity in human neurons differentiated from embryonic stem cells *via* mitochondrial apoptosis pathway. Curr Drug Saf. 2012;7(2):106-119.
DOI: 10.2174/157488612802715663.
69. Slikker Jr W, Liu F, Rainosek SW, Patterson TA, Sadovova N, Hanig JP, *et al*. Ketamine-induced toxicity in neurons differentiated from neural stem cells. Mol Neurobiol. 2015;52(2):959-969.
DOI: 10.1007/s12035-015-9248-5.
70. Félix LM, Vidal AM, Serafim C, Valentim AM, Antunes LM, Monteiro SM, *et al*. Ketamine induction of p53-dependent apoptosis and oxidative stress in zebrafish (Danio rerio) embryos. Chemosphere. 2018;201:730-739.
DOI: 10.1016/j.chemosphere.2018.03.049.
71. Bai X, Yan Y, Canfield S, Muravyeva MY, Kikuchi C, Zaja I, *et al*. Ketamine enhances human neural stem cell proliferation and induces neuronal apoptosis via reactive oxygen species-mediated mitochondrial pathway. Anesth Analg. 2013;116(4):869-880.
DOI: 10.1213/ANE.0b013e3182860fc9.
72. Motaghinejad M, Motevalian M, Fatima S, Faraji F, Mozaffari S. The neuroprotective effect of curcumin against nicotine-induced neurotoxicity is mediated by CREB-BDNF signaling pathway. Neurochem Res. 2017;42(10):2921-2932.
DOI: 10.1007/s11064-017-2323-8.
73. Motaghinejad M, Karimian M, Motaghinejad O, Shabab B, Yazdani I, Fatima S. Protective effects of various dosage of curcumin against morphine induced apoptosis and oxidative stress in rat isolated hippocampus. Pharmacol Rep. 2015;67:230-235.
DOI: 10.1016/j.pharep.2014.09.006.
74. Kandezi N, Mohammadi M, Ghaffari M, Gholami M, Motaghinejad M, Safari S. Novel insight to neuroprotective potential of curcumin: a mechanistic review of possible involvement of mitochondrial biogenesis and PI3/Akt/GSK3 or PI3/Akt/CREB/BDNF signaling pathways. Int J Mol Cell Med. 2020;9(1):1-32.
DOI: 10.22088/IJMCM.BUMS.9.1.1
75. Motaghinejad M, Bangash MY, Hosseini P, Karimian SM, Motaghinejad O. Attenuation of morphine withdrawal syndrome by various dosages of curcumin in comparison with clonidine in mouse: possible mechanism. Iran J Med Sci. 2015;40(2):125-132.
PMID: 25821292.

76. Aggarwal BB, Harikumar KB. Potential therapeutic effects of curcumin, the anti-inflammatory agent, against neurodegenerative, cardiovascular, pulmonary, metabolic, autoimmune and neoplastic diseases. Int J Biochem Cell Biol. 2009;41(1):40-59. DOI: 10.1016/j.biocel.2008.06.010.
77. Cole GM, Teter B, Frautschy SA. Neuroprotective effects of curcumin. Adv Exp Med Biol. 2007;595:197-212. DOI: 10.1007/978-0-387-46401-5_8.
78. Darvesh AS, Carroll RT, Bishayee A, Novotny NA, Geldenhuys WJ, Van der Schyf CJ. Curcumin and neurodegenerative diseases: a perspective. Expert Opin Investig Drugs. 2012;21(8):1123-1140. DOI: 10.1517/13543784.2012.693479.
79. Huang HC, Chang P, Dai XL, Jiang ZF. Protective effects of curcumin on amyloid-β-induced neuronal oxidative damage. Neurochem Res. 2012;37(7):1584-1597. DOI: 10.1007/s11064-012-0754-9.
80. Huang HC, Xu K, Jiang ZF. Curcumin-mediated neuroprotection against amyloid-β-induced mitochondrial dysfunction involves the inhibition of GSK-3β. J Alzheimers Dis. 2012;32(4):981-096. DOI: 10.3233/JAD-2012-120688.
81. Liu L, Zhang W, Wang L, Li Y, Tan B, Lu X, *et al*. Curcumin prevents cerebral ischemia reperfusion injury via increase of mitochondrial biogenesis. Neurochem Res. 2014;39(7):1322-1331. DOI: 10.1007/s11064-014-1315-1.
82. Gera M, Sharma N, Ghosh M, Huynh DL, Lee SJ, Min T, *et al.* Nanoformulations of curcumin: an emerging paradigm for improved remedial application. Oncotarget. 2017;8(39):66680-66698. DOI: 10.18632/oncotarget.19164.
83. Ghalandarlaki N, Alizadeh AM, Ashkani-Esfahani S. Nanotechnology-applied curcumin for different diseases therapy. Biomed Res Int. 2014;2014:394264,1-23. DOI: 10.1155/2014/394264.
84. Yu Y, Shen Q, Lai Y, Park SY, Ou X, Lin D, *et al*. Anti-inflammatory effects of curcumin in microglial cells. Front Pharmacol. 2018;9:386,1-10. DOI: 10.3389/fphar.2018.00386.
85. Shehzad A, Rehman G, Lee YS. Curcumin in inflammatory diseases. Biofactors. 2013;39(1):69-77. DOI: 10.1002/biof.1066.
86. Bagheri H, Ghasemi F, Barreto GE, Rafiee R, Sathyapalan T, Sahebkar A. Effects of curcumin on mitochondria in neurodegenerative diseases. Biofactors. 2020;46(1):5-20. DOI: 10.1002/biof.1566.
87. Trujillo J, Granados-Castro LF, Zazueta C, Andérica-Romero AC, Chirino YI, Pedraza-Chaverrí J. Mitochondria as a target in the therapeutic properties of curcumin. Arch Pharm (Weinheim). 2014;347(12):873-884. DOI: 10.1002/ardp.201400266.
88. Salehi B, Stojanović-Radić Z, Matejić J, Sharifi-Rad M, Kumar NVA, Martins N, *et al*. The therapeutic potential of curcumin: a review of clinical trials. Eur J Med Chem. 2019;163:527-545. DOI: 10.1016/j.ejmech.2018.12.016.
89. Mohseni M, Sahebkar A, Askari G, Johnston TP, Alikiaii B, Bagherniya M. The clinical use of curcumin on neurological disorders: an updated systematic review of clinical trials. Phytother Res. 2021;35(12):6862-6882. DOI: 10.1002/ptr.7273.